coatings

MDPI

Article

Highly Bioactive Elastomeric Hybrid Nanoceramics for Guiding Bone Tissue Regeneration

Jing Chen [1,2,*], Wenxiu Que [2,*], Bo Lei [3] and Beibei Li [1]

[1] The Key Laboratory for Surface Engineering and Remanufacturing in Shaanxi Province, School of Chemical Engineering, Xi'an University, Xi'an 710065, China
[2] Electronic Materials Research Laboratory, International Center for Dielectric Research, Key Laboratory of the Ministry of Education, School of Electronic & Information Engineering, Xi'an Jiaotong University, Xi'an 710054, China
[3] Frontier Institute of Science and Technology, Xi'an Jiaotong University, Xi'an 710054, China
* Correspondence: jingchen@xawl.edu.cn (J.C.); wxque@mail.xjtu.edu.cn (W.Q.); Tel./Fax: +86-29-83385679 (W.Q.)

Abstract: Conventional bioactive ceramic implants possess high osteogenic ability but exhibit poor machinability and brittleness, which limit their wide applications. In this study, we report an elastomeric machinable bioactive nanoceramic-based hybrid membrane that is formed by nanohydroxyapatite-reinforced hybrid matrix (poly(dimethylsilicone)-bioactive glass-poly(caprolactone) (nHA-PBP)) using a modified sol-gel process. The hybrid matrix is composed of elastomeric polydimethylsiloxane and bioactive glass nanogel. The effect of the nHA contents (0, 20, 30, 40 and 50 wt%) on the physicochemical structure and biomineralization activity of PBP hybrid membranes is investigated systematically. The results show that nHA-PBP hybrid membranes containing more than 20 wt% nHA exhibit the highest apatite-forming bioactivity due to the optimized hydroxyapatite crystalline phase. NHA-PBP implants with nHA also show good elastomeric mechanical behavior and foldable mechanical properties. Furthermore, the study of the in vitro cellular biocompatibility suggests that the nHA-PBP hybrid monoliths can enhance osteoblast (MC3T3-E1) attachment and proliferation. The biomimetic hybrid composition, crack-free monolith structure, and high biological activity of apatite formation make the nHA-PBP hybrid membrane a prospective candidate in the application of bone tissue regeneration.

Keywords: bioactive materials; bioactive ceramic; bioactive glass; nanohydroxyapatite; sol-gel process

check for updates

Citation: Chen, J.; Que, W.; Lei, B.; Li, B. Highly Bioactive Elastomeric Hybrid Nanoceramics for Guiding Bone Tissue Regeneration. *Coatings* **2022**, *12*, 1633. https://doi.org/10.3390/coatings12111633

Academic Editor: Jun-Beom Park

Received: 5 October 2022
Accepted: 25 October 2022
Published: 27 October 2022

Publisher's Note: MDPI stays neutral with regard to jurisdictional claims in published maps and institutional affiliations.

Copyright: © 2022 by the authors. Licensee MDPI, Basel, Switzerland. This article is an open access article distributed under the terms and conditions of the Creative Commons Attribution (CC BY) license (https://creativecommons.org/licenses/by/4.0/).

1. Introduction

Bioactive glass-based biomaterials (BGs) have shown successful applications in bone tissue repair and regeneration due to their good biocompatibility, osteoconductivity, and bone-bonding ability when implanted in vivo without any interfaces of fibrous connective tissue [1–4]. This high bone-bonding ability with living bone tissue is considered to be highly associated with their bone-like apatite layer formation [5]. Because BG has a high conductivity and bone bondability, and enhanced bone regeneration potential, the application of BG-based biomaterials in bone tissue regeneration has widely attracted attention in recent years [6]. However, pure BG is limited for use in bone tissue engineering applications due to its inherent brittleness and low flexibility. Furthermore, it is difficult for BG to form various shapes for improving in vivo applications. Hence, there is a considerable need to design and fabricate highly bioactive glass-based biomaterials with tough mechanical properties for bone tissue engineering applications.

As compared with inorganic bioactive glass materials, biopolymers exhibit unique biological physical and biochemical properties, such as high toughness, electrometric properties, greater capacity for body fluid absorption, and better gel forming capacity [7]. Hence, it is reasonable to incorporate inorganic nanoparticles into a polymer matrix to produce nanocomposites with optimized physicochemical properties, such as bioactive

glass micro-nanoscale particles-poly(caprolactone) (MNBG-PCL) biomaterials [8,9]. Actually, the addition of bioactive phases significantly improves the mechanical modulus, biomineralization activity, and biocompatibility in osteoblasts of the PCL matrix [10–12], but a particle-based inorganic phase is an obstacle to the enhancement of the strength and toughness of the polymer simultaneously due to its poor interactions [13]. Recently, molecular-level-based silica-based glass sol was added into a polymer solution to synthesize the bioactive glass–polymer hybrid biomaterials, including BG-PCL, BG-gelatin, BG-chitosan, and BG-poly(ethylene glycol) [14–16]. In the case of the molecular hybridization, the obtained hybrids show the stable mechanical property, biomineralization activity, and osteoblast biocompatibility. As a result, the development of silica-based hybrid polymer biomaterials for effective bone tissue regeneration applications is highly promising [17].

In the guiding bone tissue regeneration application, the guiding membrane biomaterials are crucial to enhance the tissue repair through preventing the invasion of external protein and cells [18]. The ideal guiding membrane should be tough, bioactive, and easy-handling. In our previous work, poly(dimethylsilicone)-bioactive glass-PCL (PBP) hybrid membranes without fracture were successfully fabricated via a sol-gel process, which exhibited a controlled surface morphology, mechanical property, and biomineralization [10]. There is still much space to improve the apatite-forming ability (biomineralization activity) and osteoblast biocompatibility of the PBP hybrid membrane. Human bone tissue is a typical organic–inorganic composite consisting of nano-crystalline hydroxyapatite (nHA) and collagen polymer. Artificial HA has received more attention as a bioactive ceramic material in bone replacement and repair applications due to its similar structure and composition to natural apatite. It was selected as an inorganic additive for biomimicking. In addition, some published works suggest that HA supplementation can provide pH buffers for acid-released production [19–21]. In this regard, incorporating nanoscale HA into biomaterials may be a promising option for enhancing biomineralization activity and osteoblastic ability.

In this study, the crack-free nHA-PBP hybrid membranes are prepared via a typical sol-gel method. The effects of the addition of nanoscale HA (nHA) on the structural property and biomineralization activity of the PBP hybrids are also investigated. In addition, the purpose of this study is to analyze the effects of nHA-PBP hybrid membranes with different HA loading concentrations on cell attachment to examine the basic biocompatibility of hybrid materials. It is anticipated that the incorporation of nHA can significantly improve the biomineralization and osteoblastic biocompatibility of the nHA-PBP hybrid biomaterials.

2. Experimental

2.1. Materials

Tetraethoxysilane (TEOS, $Si(OC_2H_5)_4$), calcium nitrite ($Ca(NO_3)_2{\cdot}4H_2O$), isopropyl-alcohol (IPA), tetrahydrofuran (THF), dichloromethane (DCM), and hydrochloric acid (HCl, 35%) were obtained from Guanghua Chemical Factory Co., Ltd. (Guangzhou, China). Polydimethylsiloxane (PDMS, $HO\text{-}[Si(CH_3)_2\text{-}O\text{-}]_nH$, Mn = 1100) was provided by Alfa (Alfa, Ward Hill, MA, USA). Poly(caprolactone) (PCL, $(C_6H_{10}O_2)_n$) (M_n = 80,000) was supplied by Sigma-Aldrich (Sigma-Aldrich, St. Louis, MO, USA). Nano-hydroxyapatite (nHA) powder (consisting of loose aggregates of approximately 100 nm crystals) was purchased from Alfa Aesar (Ward Hill, MA, USA)

2.2. Synthesis of nHA-PBP Hybrid Membrane

The nHA-PBP hybrid membranes were synthesized. Briefly, 10 mL IPA and 20 mL THF were combined to form co-blended solvents, TEOS (6.5 g) was first dissolved in this aqueous solution. Thirty minutes later, 1.5 mL of 35% HCL, 12 mL of water, and 2.2 g of PDMS were added into the solution for completely catalyzation and hydrolyzed reaction for 30 min. Then, the $Ca(NO_3)_2{\cdot}4H_2O$, IPA, and H_2O were added to the aforementioned solution. The generated bioactive PDMS-BG sol was then mixed with the DCM solution of PCL and further stirred for 30 min. To obtain the nHA-PBP hybrid sol, the predetermined

containing nHA (0, 20, 30, 40, and 50 wt% relative to the PCL polymer) was added and vigorously stirred for 20 h. Then, the mixture was poured into the Teflon dishes and dried at 37 °C for 12 h to form the nHA-PBP mixed gel. Finally, after heating the mixed gel at 60 °C for 12 h, the nHA-PBP hybrid membranes were obtained.

2.3. Characterization of the Specimens

Scanning electron microscopy (SEM, JSM-6390, JEOL, Tokyo, Japan) was used to characterize the surface microstructural and morphological properties of samples. The elemental composition of the samples was evaluated by energy dispersive spectrometry (EDS, JEOL, Tokyo, Japan). The crystalline phase structure of the hybrid membranes were studied through Cu Kα radiation measured by X-ray diffraction of radiation, performed at 40 kV and 30 mA; the scanning speed was 0.02°/s and the step size was 0.02°, ranging from 15° to 60° (XRD, D/MAX-2400, Rigaku, Tokyo, Japan).

2.4. Mechanical Behavior Assessment of Hybrids

The universal mechanical devices (SHT4206, MTS, Minneapolis, MN, USA) with a 500 N load cell was used to evaluate the tensile mechanical characteristics (tensile strength and modulus) of hybrid monoliths at a crosshead speed of 50 mm per minute. All samples with a size of 10 mm × 60 mm were used for the tensile mechanical test. The stress–strain curves were captured by the additional software of the machine. The tensile modulus of samples was obtained by determining the slope of the initial linear elastic portion of stress–strain curves. At least five species were counted in each sample.

2.5. Biomineralization Activity

According to our previous report, the specimens incubated in simulated body fluid (SBF) for a certain time to determine the biomineralization activity of hybrid membranes [22]. After soaking, the formation of apatite on the surface of the sample was tested. Briefly, the samples were cut into a size of 10 × 10 × 2 mm^3 and incubated in SBF with a similar composition to human blood plasma (in mM: Ca^{2+} 2.5, Mg^{2+} 1.5, Na^+ 142, K^+ 5.0, $SO_4{}^{2-}$ 0.5, $HPO_4{}^{2-}$ 1.0, Cl^- 147.8, $HCO_3{}^-$ 4.2). After 7 days of incubation at 37 °C, the samples were taken out of the fluids and washed with deionized water to remove the specimen. Then, the samples were dried at 40 °C for 24 h. Then, the activity of apatite forming on the surface of the samples was analyzed by SEM, EDS, and XRD.

2.6. Cell Proliferation and Viability of the Hybrid Membranes

The cellular biocompatibility of the hybrid membrane was evaluated by using the osteoblast cell line (MC3T3-E1). Cells were cultured in a standard Dulbecco's modified essential medium (DMEM, Invitrogen) in a humidified atmosphere with 5% CO_2 and supplemented with 10% fetal calf serum (FCS). All samples with a size of 10 mm × 10 mm were sterilized by ultraviolet (UV) irradiation for 30 min on each side before cell seeding. MC3T3-E1 cells were seeded on the surface of the hybrid materials at a density of 5000 cells per well. The cell attachment and morphology were then evaluated with a LIVE/DEAD viability kit (Molecular Probes) after the 3-day culture. The staining procedure was according to the manufacture instruction. The cell morphology was observed with a fluorescence microscope (IX53, Olympus, Tokyo, Japan).

After the incubation for 1, 3, and 5 days, the cell viability and proliferation were determined by using a commercial Alamar Blue™ assay kit (Life Technologies). A tissue culture plate (TCP) was used as a control. The cell metabolic activity after incubation with an Alamar Blue kit was performed by a microplate reader (Molecular Devices) according to the instruction book. At least 5 species per sample were analyzed to obtain mean value and standard deviation (SD).

2.7. Statistics Analysis

Mean ± standard deviation (SD) indicated all data. The student's test analysis of Social Science Statistical Program Software (SPSS 19.0, Inc., Chicago, IL, USA) used to detect the statistical differences between the groups of measurements. Statistically significant difference was represented as * p less than 0.05 and ** p less than 0.01.

3. Results and Discussion

3.1. Morphological Measurement

Through the direct hybridization of PDMS-BG sol, PCL solution, and nHA, the nHA-PBP hybrids were successfully obtained as shown in Figure 1. After thermal casting and incubation, the crack-free hybrid membrane formed. In the hybrid structure, PDMS may have a strong interaction with BG sol through the Si-O-Si bonds. Furthermore, the hydrophobic alkyl chains may have high affinity with the PCL phase. Therefore, the molecular-level inorganic–organic phase structure of the as-fabricated hybrid membranes can be facilely formed. In addition, the nanoscale HA particles are efficiently incorporated into the PBP matrix, which may enhance their surface nanostructure and bioactivity, as well as the osteoblasts biocompatibility.

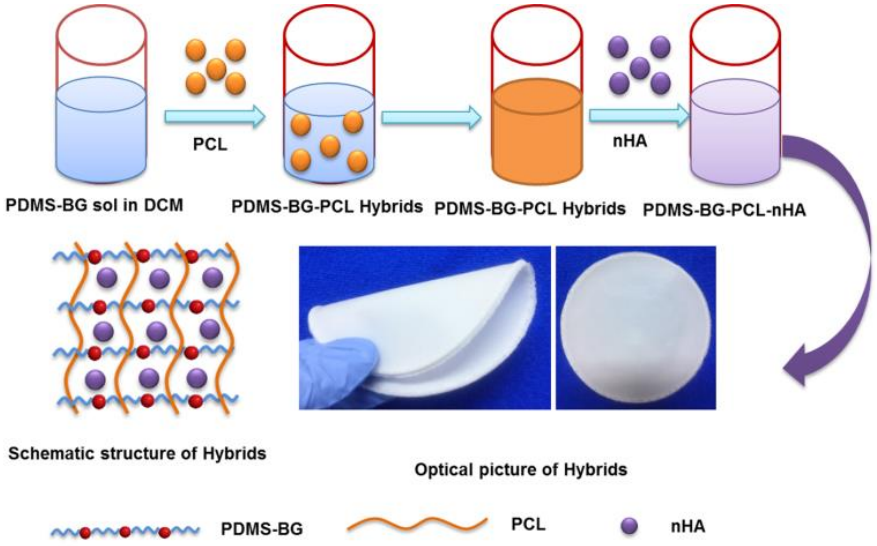

Figure 1. Process diagram and optical images of crack-free nHA-PBP hybrid monoliths fabricated by the representative sol-gel route.

Figure 2 reveals the crystalline phase composition and structure of the as-fabricated nHA-PBP hybrids with various amounts of nHA (0, 20, 30, 40, and 50 wt%) by XRD characterization. In spite of the variations observed in crystallization, one can clearly observe the XRD peaks at $2\theta = 21.88°$ and $2\theta = 23.85°$, which are ascribed to the representative characteristic peaks of the PCL (semi-crystalline polymer). It is also observed that the PCL peaks significantly decrease in intensity with the increase in nHA content (20–50 wt%). Furthermore, the appearance and significant enhancement in intensity of the peaks at 32°, 46°, and 49° demonstrates the presence of nHA in the nHA-PBP hybrids.

The surface microstructures and morphologies of the nHA-PBP hybrid membranes containing different nHA contents are shown in Figure 3. It can be observed that the surface roughness of the hybrids increases significantly with the addition of nHA. There are some joints and protuberances on the surface of these composites, which indicates that HA nanoparticles are attached to PCL surfaces. The SEM images also show that the HA particles (particle areas) density increases when the loading concentration increases (Figure 3C–E). Figure 4 shows EDS spectra of the nHA-PBP hybrid membranes. The results confirm that calcium (Ca), phosphorous (P), carbon (C), and oxygen (O) are present in

the matrix. The diagram demonstrates that the chemical composition changes with the addition of different nHA contents. The Ca and P peaks in intensity significantly rise with the increase in nHA content. These results reveal that nHA can be effectively crosslinked and hybridized with the PBP matrix.

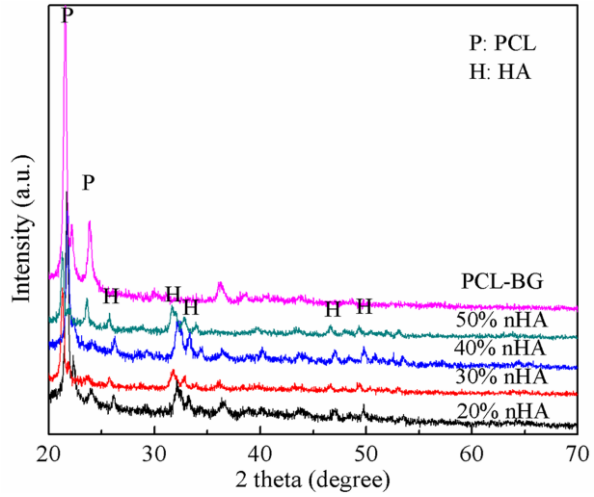

Figure 2. XRD patterns of the nHA-PBP hybrid membranes with different nHA contents.

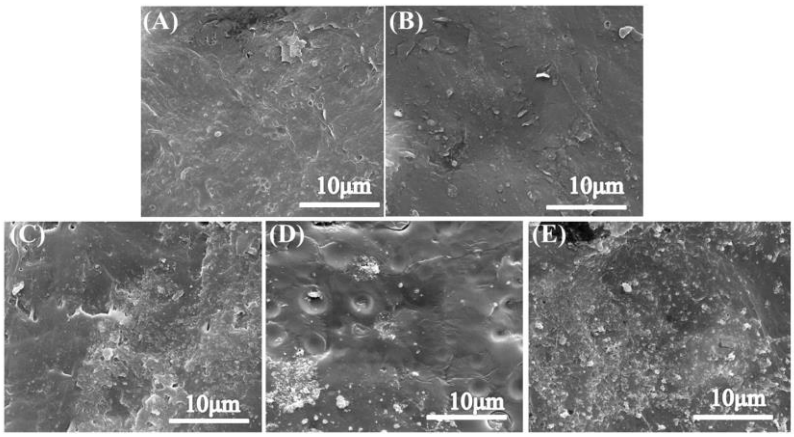

Figure 3. Surface microstructures and morphologies of the nHA-PBP hybrid membranes. (**A**) 0 wt% nHA, (**B**) 20 wt% nHA, (**C**) 30 wt% nHA, (**D**) 40 wt% nHA, (**E**) 50 wt% nHA.

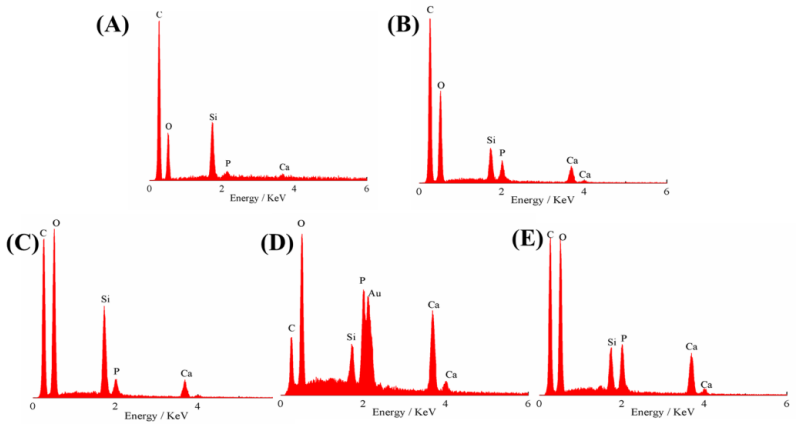

Figure 4. EDS analysis spectra of the nHA-PBP hybrid membranes. (**A**) 0 wt% nHA, (**B**) 20 wt% nHA, (**C**) 30 wt% nHA, (**D**) 40 wt% nHA, (**E**) 50 wt% nHA.

3.2. Mechanical Properties Assessment of the nHA-PBP Hybrid Membranes

The tensile tests are used to assess the mechanical properties of nHA-PBP hybrid membranes, as shown in Figure 5. Figure 5A shows the tensile stress–strain behavior of nHA-PBP hybrids with varying nHA contents (20, 30, 40 wt%). All samples show representative stress–strain behaviors in the initial 10% stain range. The ultimate tensile strength of hybrid membranes decreased from 4.77 ± 0.30 to 2.77 ± 0.25 MPa with increasing nHA content from 20 to 40 wt% (Figure 5B). The Young's modulus of nHA-PBP 20 wt% hybrids indicated a high value of 87.94 ± 1.32 MPa as compared to the 59.58 ± 2.54 of 40 wt% (Figure 5C). The failure stress showed a similar tendency to change with ultimate tensile strength for nHA-PBP from 20 to 40 wt% (Figure 5D). The results show that increasing the amount of nHA in the nHA-PBP hybrids reduced flexural strength. When the nHA content is high, the nHA may not be hybridized well with the polymer phase, and the uniform structure may induce the decrease in flexural strength. Since nHA has poor mechanical properties, its utilization is limited to clinical load bearing applications. To make nHA-PBP hybrid materials play an important role in bone regeneration, some weaknesses of each component need to be improved in order to provide excellent quality and interfacial attachment of new bone tissue.

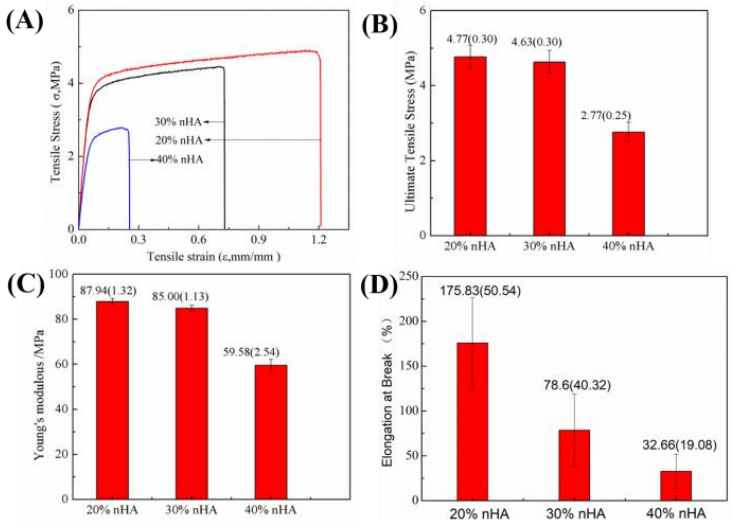

Figure 5. Mechanical properties assessment of nHA-PBP hybrid membranes with different nHA contents. (**A**) Stress–strain behavior; (**B**) Ultimate tensile strength; (**C**) Young's modulus; (**D**) Elongation at break.

3.3. Biomineralization Activity of the nHA-PBP Hybrid Membranes

Considering that the biomineralization activity critically influences the biomaterials in bone tissue regeneration, here, the bioactivity of the nHA-PBP hybrid membranes for in vitro apatite forming is assessed by immersion in SBF for 7 days. As shown in Figure 6, the apatite formation capability of the hybrid membranes is significantly affected by the nHA contents. As one can see in Figure 6, the surface of the nHA-PBP hybrid membranes shows new apatite layers relative to the specimens before incubation in SBF (in Figure 3). That is, the mineral is deposited and aggregated in the form of a globular accumulation on the surface of the sample with 0 wt% nHA of the nHA-PBP hybrid membranes as in Figure 6A,B. When the additive of nHA increases to 20 wt% and 30 wt%, the nHA-PBP is covered with densely spherically shaped particles as seen in Figure 6C–F. With the nHA content increasing, the surface morphology of the as-formed hydroxyapatite nanocrystals changes considerably. In addition, it progressively shows needle-like or rod-like characteristics in shape, as shown in Figure 6H,J, showing typical biomineralization characteristics only for bioactive glass materials.

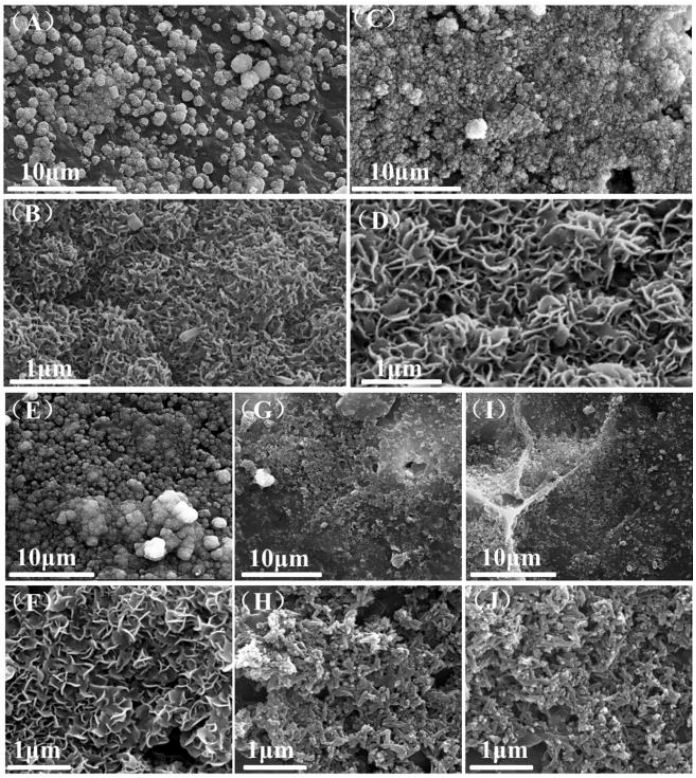

Figure 6. Surface morphologies of the nHA-PBP hybrid membranes with different nHA contents after biomineralization in SBF for 7 days. (**A**,**B**) 0 wt% nHA, (**C**,**D**) 20 wt% nHA, (**E**,**F**) 30 wt% nHA, (**G**,**H**) 40 wt% nHA, (**I**,**J**) 50 wt% nHA.

Figure 7 shows the EDS spectra of the nHA-PBP hybrid membranes with various nHA contents after being immersed into SBF for 7 days. It can be seen that, compared to the EDS of the hybrid membrane before being soaked, immersion into SBF leads to the formation of the hydroxyapatite. As the nHA content increases, the formation of hydroxyapatite increases, which is accordant with the published literature. In addition, EDS of the hybrid membrane with the addition of 20 wt% nHA, after being soaked in SBF, shows a significant decrease in the calcium content, indicating a biological apatite formation with a calcium-deficient characteristic [23].

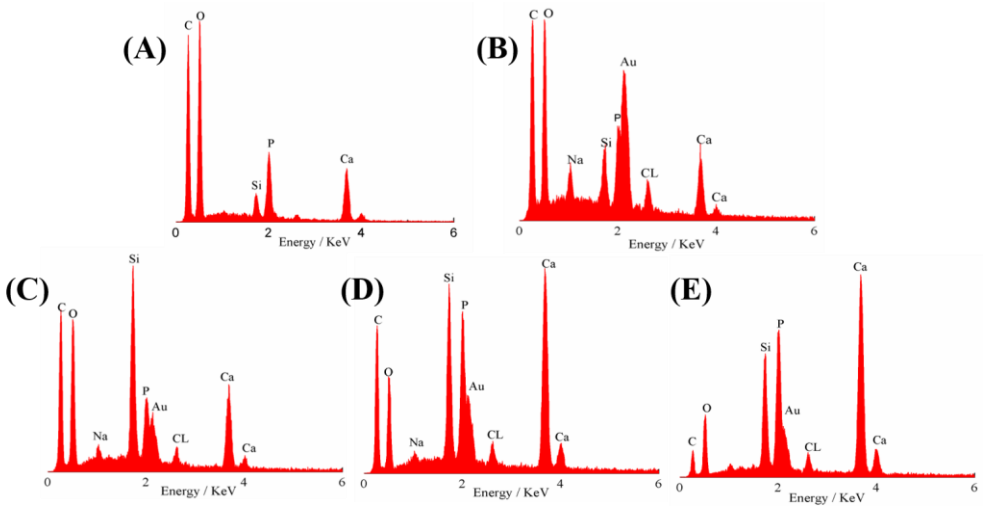

Figure 7. Elemental compositions of the nHA-PBP hybrid membranes with different nHA contents after biomineralization in SBF for 7 days. (**A**) 0 wt% (**B**) 20 wt%; (**C**) 30 wt%; (**D**) 40 wt%; (**E**) 50 wt%.

Figure 8 shows the XRD patterns of the hybrid membranes containing different nHA contents and after the 7 days of incubation in SBF, which are employed to investigate the structure of the crystalline phase property of the new forming apatite layer on the hybrid membrane surface. These results indicate that several characteristic peaks are related to crystalline hydroxyapatite. It is also clear to see that the peaks referring to PCL at $2\theta = 21.88^\circ$ and $2\theta = 23.85^\circ$ are significantly weakened in intensity after 7 days of soaking in SBF, which implies the newly mineralized apatite layer forming on the specimens film. The XRD diffraction peaks at 32°, 39°, 46°, and 49° for the hybrids with the addition of 20–50 wt% of nHA correspond to the crystal planes of (211), (310), (222), and (213) of the HA (JCPDS No. 09-0432) [21]. It should be noted that the characteristic peaks of HA are not obvious for the pure PBP hybrid. Clearly, these SEM, EDS, and XRD results demonstrate that the nHA incorporation can remarkably increase the capability for biomineralization in the nHA-PBP hybrid membranes.

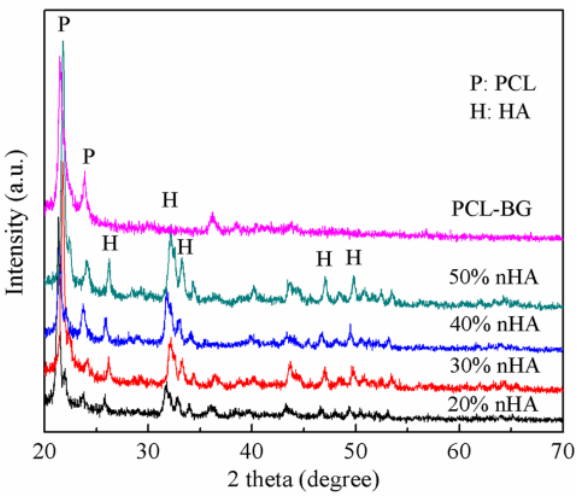

Figure 8. XRD patterns of the nHA-PBP hybrid membranes with different nHA contents after biomineralization in SBF for 7 days. Representative diffraction peaks of hydroxyapatite were marked in the patterns.

3.4. Osteoblasts Biocompatibility Assessment of the nHA-PBP Hybrid Membranes

Figure 9 shows the cell attachment and proliferation activity of the osteoblast line (MC3T3-E1) after culturing for 1, 3, and 5 days on the surface of the hybrid membranes. The cells show normal attachment and spreading morphology on the surface of the PBP hybrid membrane, as shown in Figure 9A. While for the nHA-PBP 20 wt% (in Figure 9B) and the nHA-PBP 50 wt% (in Figure 9C) after being cultured for 5 days, there are no significant dead cells observed on the surface of these samples, demonstrating their good cell attachment ability. There are high cell numbers on the surfaces of the hybrid membrane with the incorporation of 20 wt% and 50 wt% nHA compared to the pure PBP hybrid membrane, further suggesting their enhanced cellular biocompatibility. In addition, the cell viability on the PCL and the nHA-PBP hybrid membranes significantly increases as the culture period extends from 1 day to 5 days, which indicates that the as-fabricated hybrid membranes can support the osteoblast proliferation, as seen in Figure 9D. Compared to the PBP control, the osteoblast presents significantly high cell viability after incubating with the nHA-PBP (20% and 50%) for 5 day culture periods. The cell viability is significantly improved as the nHA incorporation increases. These results demonstrate that our nHA-PBP hybrid membranes possess a good osteoblast biocompatibility and the incorporation of nHA can efficiently improve the osteoblast activity of the PBP hybrid membranes.

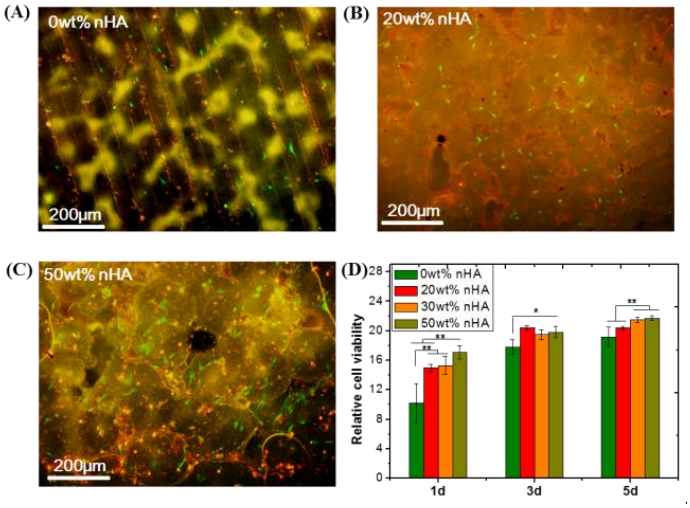

Figure 9. Osteoblasts biocompatibility investigation of the nHA-PBP hybrid membranes with different nHA contents (20 wt% and 50 wt% nHA). MC3T3-E1 cell attachment morphology at 3 days ((**A**), 0 wt%, (**B**), 20 wt% and (**C**), 50 wt% nHA) and proliferation activity after 1–5 days of culture (**D**). * $p < 0.05$ and ** $p < 0.01$ represent the significance differences between groups (n = 5).

In our previous work, the crack-free PBP hybrid membrane was successfully prepared by a conventional sol-gel method, which developed the functional hybrid membranes by incorporating HA particles into PBP sol. The relation between the hybrid properties and apatite-forming bioactivity was investigated, as well as attachment and proliferation in vitro. As one knows, PDMS is well compatible with silicon-based sol phase because it has a typical Si-O-Si skeleton chain and side chain, which induces a strong interaction with the hydrophobic PCL polymer. However, the biomineralization capability and biocompatibility of osteoblasts with the materials still need further improvement. Due to its highly biomimetic chemical structure and composition, HA is a typical bioactive ceramic and was successfully used in bone regeneration. The SEM results show that the HA particles can be uniformly dispersed into the PCL matrix. As a result, in this material system, it is easy to form a homogeneous inorganic–organic hybrid structure. The additive of nHA significantly enhances the biomineralization activity (apatite-forming ability) of the PBP hybrid membranes, as previously reported [24–26]. It is known that MC3T3-E1 cells have different reactions to changes in hybrid surface properties. The surface roughness of these two samples (i.e., 0 wt% and 20 wt% of the nHA) was not significantly different (Figure 3A,B), the number of attached cells on nHA 20 wt% was slightly higher than that of the nHA 0 wt%. This suggests that MC3T3-E1 cells prefer HA-containing samples to adhesion and proliferation. One possible explanation is that HA exists on a composite surface, resulting in more permanent interaction with adsorbed protein. It is absorbed by serums and proteins in the culture medium, or the protein is absorbed by the cell itself. It is also apparent that the cells are distributed more evenly on the nHA-PBP hybrid membrane surface (Figure 9B,C), which further suggests that HA favors the uniform distribution of adsorbed proteins. The addition of nHA also greatly enhances the osteoblasts biocompatibility of the as-fabricated PBP hybrid membranes. In addition, these results match earlier studies that reported the important role of nHA in polymer nanocomposites [27–29].

In bone tissue regeneration applications, the ideal biomaterials should be facilely synthesized and have high bioactivities, including biomineralization activity, for bone-bonding and osteoblast biocompatibility for regeneration. However, the PBP hybrid membrane needs a long processing time (more than 72 h), which is unfavorable for large-scale production and, thereby, limits applications. Based on the requirement for reducing the processing time and enhancing biomineralization activity and osteoblast biocompatibility, the present new developed nHA-PBP hybrid membranes may have promising applications in future bone tissue regeneration.

4. Conclusions

To sum up, highly bioactive and crack-free nHA-PBP hybrid membrane ingredients were successfully prepared via the conventional sol-gel method. Results indicate that adding HA can significantly improve the surface roughness and biomineralization activity of hybrid membranes. The nHA-PBP hybrid membranes after being soaked in SBF can easily induce a crystalline apatite layer on the surface, indicating their excellent biomineralization activity. The optimized nHA-PBP hybrids also show significantly enhanced osteoblast biocompatibility. The hybrids containing 20 wt% nHA show an optimized elastic modulus and toughness. The crack-free structure, short processing time, and high bioactivity of the production of hydroxyapatite formation and biomimetic hybrid composition make the as-fabricated nHA-PBP hybrid membrane a desired candidate as a guidance membrane for future applications in biomedical materials.

Author Contributions: Methodology, J.C. and B.L. (Bo Lei).; software, J.C. and B.L. (Beibei Li); investigation, J.C.; writing—original draft preparation, J.C.; writing—review and editing, J.C., B.L. (Bo Lei) and W.Q.; funding acquisition, J.C. and B.L. (Beibei Li). All authors have read and agreed to the published version of the manuscript.

Funding: This research was funded by the Natural Science Basic Research Plan in Shaanxi Province of China (No. 2019JM-520 and 2020JQ-890), the 3-year action plan of Xi'an University (2021xdjh34).

Institutional Review Board Statement: Not applicable.

Informed Consent Statement: Not applicable.

Data Availability Statement: All the data supporting the results of the study are included in the paper.

Conflicts of Interest: The authors declare no conflict of interest.

References

1. Kaur, G.; Kumar, V.; Baino, F.; Mauro, J.C.; Pickrell, G.; Evans, L.; Bretcanu, O. Mechanical properties of bioactive glasses, ceramics, glass-ceramics and composites: State-of-the-art review and future challenges. *Mater. Sci. Eng. C* **2019**, *104*, 109895.
2. Hum, J.; Boccaccini, A.R. Bioactive glasses as carriers for bioactive molecules and therapeutic drugs: A review. *J. Mater. Sci. Mater. Med.* **2012**, *23*, 2317–2333. [CrossRef]
3. Furlan, R.G.; Correr, W.R.; Russi, A.F.C.; da Costa Iemma, M.R.; Trovatti, E.; Pecoraro, É. Preparation and characterization of boron-based bioglass by sol–gel process. *J. Sol-Gel Sci. Technol.* **2018**, *88*, 181–191. [CrossRef]
4. Kaur, G.; Pandey, O.P.; Singh, K.; Homa, D.; Scott, B.; Pickrell, G. A review of bioactive glasses: Their structure, properties, fabrication and apatite formation. *J. Biomed. Mater. Res. A* **2014**, *102*, 254–274. [CrossRef] [PubMed]
5. Biswal, T. Biopolymers for tissue engineering applications: A review. *Mater. Today* **2021**, *41*, 397–402. [CrossRef]
6. Lei, B.; Guo, B.; Rambhia, K.J.; Ma, P.X. Hybrid polymer biomaterials for bone tissue regeneration. *Front. Med.* **2019**, *13*, 189–201. [CrossRef]
7. Ozdil, D.; Murat Aydin, H. Polymers for medical and tissue engineering applications. *J. Chem. Technol. Biotechnol.* **2014**, *89*, 1793–1810. [CrossRef]
8. Chen, J.; Que, W.; Xing, Y.; Lei, B. Molecular level-based bioactive glass-poly (caprolactone) hybrids monoliths with porous structure for bone tissue repair. *Ceram. Int.* **2015**, *41*, 3330–3334. [CrossRef]
9. Lei, B.; Shin, K.H.; Noh, D.Y.; Jo, I.H.; Koh, Y.H.; Kim, H.E.; Kim, S.E. Sol–gel derived nanoscale bioactive glass (NBG) particles reinforced poly (ε-caprolactone) composites for bone tissue engineering. *Mater. Sci. Eng. C* **2013**, *33*, 1102–1108. [CrossRef]
10. Chen, J.; Du, Y.; Que, W.; Xing, Y.; Lei, B. Content-dependent biomineralization activity and mechanical properties based on polydimethylsiloxane–bioactive glass–poly(caprolactone) hybrids monoliths for bone tissue regeneration. *RSC Adv.* **2015**, *5*, 61309–61317. [CrossRef]
11. Pires, L.S.O.; Fernandes, M.H.F.V.; de Oliveira, J.M.M. Crystallization kinetics of PCL and PCL–glass composites for additive manufacturing. *J. Therm. Anal. Calorim.* **2018**, *134*, 2115–2125. [CrossRef]
12. Mohammadkhah, A.; Marquardt, L.M.; Sakiyama-Elbert, S.E.; Day, D.E.; Harkins, A.B. Fabrication and characterization of poly-(ε)-caprolactone and bioactive glass composites for tissue engineering applications. *Mater. Sci. Eng. C* **2015**, *49*, 632–639. [CrossRef] [PubMed]
13. Ma, J.; Wu, C. Bioactive inorganic particles-based biomaterials for skin tissue engineering. *Exploration* **2022**, *2*, 20210083. [CrossRef]
14. Sohrabi, M.; Eftekhari Yekta, B.; Rezaie, H.; Naimi-Jamal, M.R.; Kumar, A.; Cochis, A.; Miola, M.; Rimondini, L. Enhancing Mechanical Properties and Biological Performances of Injectable Bioactive Glass by Gelatin and Chitosan for Bone Small Defect Repair. *Biomedicine* **2020**, *8*, 616. [CrossRef] [PubMed]

15. Erol-Taygun, M.; Unalan, I.; Idris, M.I.B.; Mano, J.F.; Boccaccini, A.R. Bioactıve Glass-Polymer Nanocomposites for Bone Tıssue Regeneration Applicatıons: A Revıew. *Adv. Eng. Mater.* **2019**, *21*, 1900287. [CrossRef]
16. Chen, J.; Que, W.; Xing, Y.; Lei, B. Highly bioactive polysiloxane modified bioactive glass-poly (ethylene glycol) hybrids monoliths with controlled surface structure for bone tissue regeneration. *Appl. Surf. Sci.* **2015**, *332*, 542–548. [CrossRef]
17. Wu, W.; Wang, W.; Li, J. Star polymers: Advances in biomedical applications. *Progress Polym. Sci.* **2015**, *46*, 55–85. [CrossRef]
18. Gao, W.; Xiao, Y. Advances in cell membrane-encapsulated biomaterials for tissue repair and regeneration. *Appl. Mater. Today* **2022**, *26*, 101389. [CrossRef]
19. Tavakol, S.; Azami, M.; Khoshzaban, A.; Ragerdi Kashani, I.; Tavakol, B.; Hoveizi, E.; Rezayat Sorkhabadi, S.M. Effect of laminated hydroxyapatite/gelatin nanocomposite scaffold structure on osteogenesis using unrestricted somatic stem cells in rat. *Cell Biol. Int.* **2013**, *37*, 1181–1189. [CrossRef]
20. Kim, H.W.; Kim, H.E.; Salih, V. Stimulation of Osteoblast Responses to Biomimetic Nanocomposites of Gelatin-Hydroxyapatite for Tissue Engineering Scaffolds. *Biomaterials* **2005**, *26*, 5221–5230. [CrossRef]
21. Sadeghi-Avalshahr, A.; Khorsand-Ghayeni, M.; Nokhasteh, S.; Mahdavi Shahri, M.; Molavi, A.M.; Sadeghi-Avalshahr, M. Effects of hydroxyapatite (HA) particles on the PLLA polymeric matrix for fabrication of absorbable interference screws. *Polym. Bull.* **2018**, *75*, 2559–2574. [CrossRef]
22. Chen, J.; Que, W.; He, Z.; Zhang, X. PDMS-modified CaO-SiO_2 hybrids derived by a sol–gel process for biomedical applications. *Polym. Compos.* **2014**, *35*, 1193–1197. [CrossRef]
23. Hutchens, S.A.; Benson, R.S.; Evans, B.R.; O'Neill, H.M.; Rawn, C.J. Biomimetic synthesis of calcium-deficient hydroxyapatite in a natural hydrogel. *Biomaterials* **2006**, *27*, 4661–4670. [CrossRef]
24. Zhang, Y.; Reddy, V.J.; Wong, S.Y.; Li, X.; Su, B.; Ramakrishna, S.; Lim, C.T. Enhanced biomineralization in osteoblasts on a novel electrospun biocomposite nanofibrous substrate of hydroxyapatite/collagen/chitosan. *Tissue Eng. Part A* **2010**, *16*, 1949–1960. [CrossRef]
25. Altamura, D.; Pastore, S.G.; Raucci, M.G.; Siliqi, D.; De Pascalis, F.; Nacucchi, M.; Ambrosio, L.; Giannini, C. Scanning Small- and Wide-Angle X-ray Scattering Microscopy Selectively Probes HA Content in Gelatin/Hydroxyapatite Scaffolds for Osteochondral Defect Repair. *ACS Appl. Mater. Interfaces* **2016**, *8*, 8728–8736. [CrossRef]
26. Li, M.; Liu, W.; Sun, J.; Xianyu, Y.; Wang, J.; Zhang, W.; Zheng, W.; Huang, D.; Di, S.; Long, Y.-Z. Jiang, X. Culturing Primary Human Osteoblasts on Electrospun Poly (lactic-co-glycolic acid) and Poly (lactic-co-glycolic acid)/Nanohydroxy apatite Scaffolds for Bone Tissue Engineering. *ACS Appl. Mater. Interfaces* **2013**, *5*, 5921–5926. [CrossRef] [PubMed]
27. Perssona, M.; Loritea, G.S.; Kokkonena, H.E.; Choc, S.W.; Lehenkari, P.P.; Skrifvars, M.; Tuukkanena, J. Effect of bioactive extruded PLA/HA composite films on focal adhesion formation of preosteoblastic cells. *Colloids Surf. B* **2014**, *121*, 409–416. [CrossRef] [PubMed]
28. Kobayashi, M.; Nihonmatsu, S.; Okawara, T.; Onuki, H.; Sakagami, H.; Nakajima, H.; Takeishi, H.; Shimada, J. Adhesion and Proliferation of Osteoblastic Cells on Hydroxyapatite-dispersed Ti-based Composite Plate. *In Vivo* **2019**, *33*, 1067–1079. [CrossRef]
29. Monmaturapoj, N.; Srion, A.; Chalermkarnon, P.; Buchatip, S.; Petchsuk, A.; Noppakunmongkolchai, W.; Mai-Ngam, K. Properties of poly (lactic acid)/hydroxyapatite composite through the use of epoxy functional compatibilizers for biomedical application. *J. Biomater. Appl.* **2017**, *32*, 088532821771578. [CrossRef]